

Short Note

The Seismicity along the Dead Sea Fault during the Last 60,000 Years

by Y. Hamiel, R. Amit, Z. B. Begin, S. Marco, O. Katz, A. Salamon, E. Zilberman, and N. Porat

Abstract Evidence for unchanging slip rate and a Gutenberg–Richter relation for earthquake distribution along the Dead Sea fault during the past 60,000 yr are presented. The evidence comes from three different segments, approximately 100 km apart, and from three different timescales: prehistoric–paleoseismic, historical, and modern (instrumental) records. The paleoseismic data are based on two different methods. In the southern Arava Valley and the northern Jordan Valley segments, the amount of normal displacement along several faults is used, while in the Dead Sea basin the appearance of brecciated beds, which are considered as seismites, is used. We found that for the southern Arava Valley segment a constant dip-slip rate of 0.5 mm/yr can explain the cumulative normal slip during the past 45,000 yr. This suggests that normal faulting is only ~10% of the total left-lateral strike-slip motion. We also found that for all three segments, the paleoseismic and historical records of strong earthquakes lie on the linear extrapolation of the frequency–magnitude relation of the instrumental record. The calculated b-values for all three segments are between 0.85 and 1, similar to other major strike-slip faults in the world. It is concluded that the Gutenberg–Richter distribution is a stable mode in the tectonic setting of the Dead Sea fault during the past 60,000 yr.

Introduction

Time-dependent seismicity has become an important topic in the evaluation of seismic hazard (see review by Steacy *et al.*, 2005). The concept implies that current seismicity should be evaluated on the backdrop of the past, short or long. Here we discuss the Late Quaternary recurrence interval of earthquakes along the Dead Sea fault (DSF). Seismic activity of the DSF has been measured for different magnitudes and timescales: tens of thousands of years (Marco *et al.*, 1996; Amit *et al.*, 2002; Begin *et al.*, 2005), thousands of years (Amit *et al.*, 1995; Leonard *et al.*, 1998; Zilberman *et al.*, 2000), hundreds of years (Migowski *et al.*, 2004), and decades (Salamon *et al.*, 2003; Begin and Steinitz, 2005). In this work, for the first time, we combine different data sets of prehistoric–paleoseismic, historical, and modern (instrumental) observations in three different segments along the DSF: the southern Arava Valley, the northern Jordan Valley, and the Dead Sea basin segments. We then calculate the slip rate and frequency–magnitude relation for these segments and discuss the recurrence interval for strong earthquake in each segment.

Tectonic Setting

The DSF is an active fault zone, forming the boundary between the Arabia and Sinai plates, stretching from the Red

Sea to the Eurasia plate (Fig. 1). Based on geological evidence and kinematic considerations, it is generally accepted that the DSF is a continental transform, along which the principal movement has been a post-Miocene 105 km left-lateral displacement (e.g., Garfunkel *et al.*, 1981; Joffe and Garfunkel, 1987).

The left-lateral slip rate along the DSF was estimated directly from displacement of geological and archaeological structures. In the central and northern Arava Valley, strike-slip rates were calculated for the past 5 m.y. by displaced alluvial fans, terraces, and streams, with resulting values between 3 and 7.5 mm/yr (Ginat *et al.*, 1998; Klinger *et al.*, 2000; Niemi *et al.*, 2001). Based on distorted beds in the Lisan Formation (70,000–14,000 yr B.P.) a slip rate of 4.7–6.5 mm/yr was suggested for the eastern Dead Sea (El-Isa and Mustafa, 1986). In the central Jordan Valley the average slip rate during the past 47 k.y. was estimated to be 4.9 mm/yr using displaced drainage systems (Ferry *et al.*, 2007). Along a north–south trending fault in the western Dead Sea, the rate during the past 30,000 yr was determined as 3.5 mm/yr (Bartov and Sagi, 2004). In the northeastern Sea of Galilee basin the minimum rate during the past 5000 yr was found to be 3 mm/yr (Marco *et al.*, 2005), and in the Missyaf segment in Syria the rate for the past 2000 yr is 7 mm/yr (Meghraoui *et al.*, 2003).

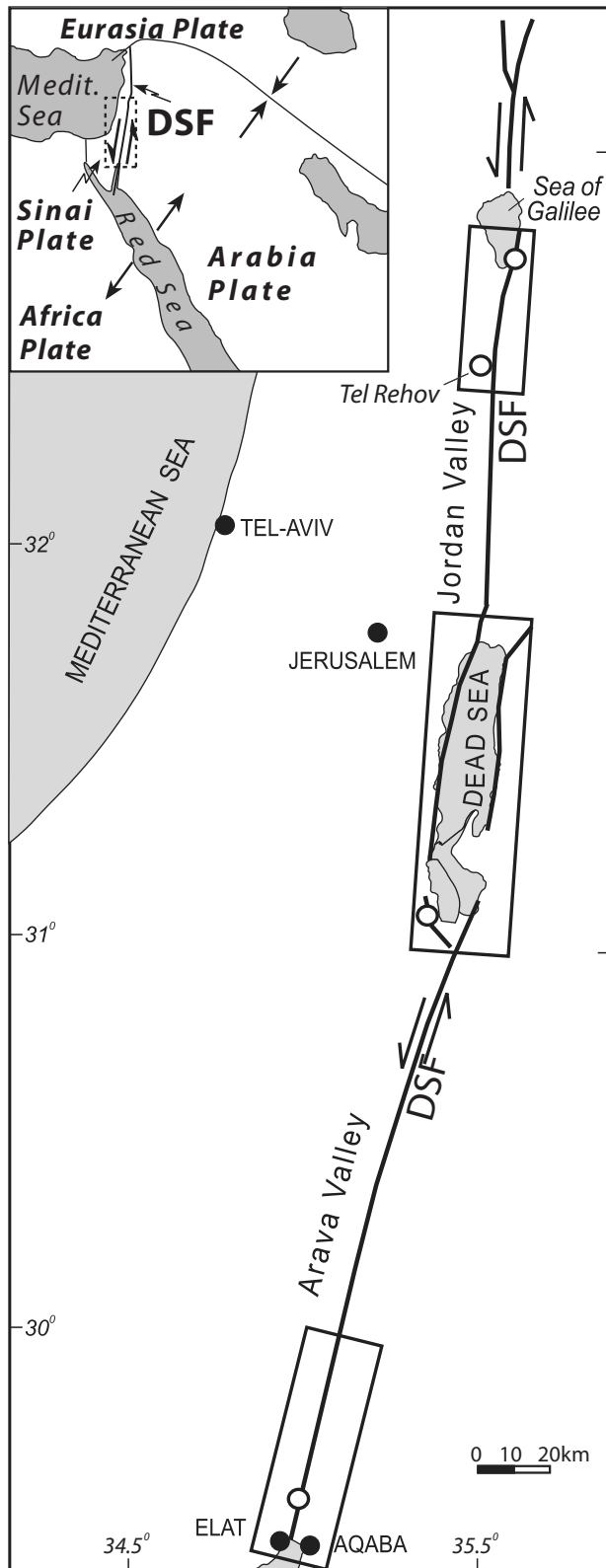


Figure 1. Location map, showing main segments along the DSF. Open circles show location of the PZ1 section of the Lisan Formation in the Dead Sea basin and locations of the study area in the southern Arava Valley and the northern Jordan Valley. Boxes denote the area considered for the instrumental record.

Along the Yammuneh segment, which strikes 30° east off the general direction of the DSF, the slip rate was determined as $3.8\text{--}6.4$ mm/yr during the past 25,000 yr (Daëron *et al.*, 2004). These field observations concerning fault displacement are generally in accord with the present rate of plate movement as measured by a Global Positioning System (GPS) and assuming a locked fault at a depth of ~ 12 km (in millimeters per year): between 5.6 ± 1 (McClusky *et al.*, 2003) and 4.4 ± 0.3 (Mahmoud *et al.*, 2005) for the southern DSF, 4.9 ± 1.4 for the Arava Valley (Le Beon *et al.*, 2008), between 3.7 ± 0.4 (Wdowinski *et al.*, 2004) and 7.5 ± 0.8 (Ostrovsky, 2001, 2005) for the central DSF in Israel, 4.4 ± 0.5 in Lebanon (Gomez *et al.*, 2007), and 6.0 ± 1 for the DSF in Syria (McClusky *et al.*, 2003).

Late Quaternary Seismicity along the Dead Sea Fault

Southern Arava Valley

Late Quaternary paleoseismicity of the southern Arava Valley was deduced from offsets on faults detected in trenches, in a fault-zone area having a surface width of 6 km and surface length of 40 km, extending through the rift valley from the northwestern coast of the Gulf of Elat (Aqaba) to the northeast (Amit *et al.*, 1995, 2002; Zilberman *et al.*, 2005). The fault zone may be subdivided into three subzones: a central subzone, 5 km wide, trending northeast, characterized by sinistral faults expressed by push-ups and pull-aparts, and two marginal zones characterized by normal faults that trend northwest and north-northeast on both sides of the rift valley. Amit *et al.* (2002) reported 20 different paleoearthquakes between 45 and 1 k.y. B.P. in the southern Arava Valley segment. The cumulative normal slip versus time that was calculated from their data (Fig. 2) shows that a constant slip rate of 0.5 mm/yr can account for the total normal slip. The relatively small amount of normal slip per event recorded during the past 16 k.y. (12 events, average slip of 0.65 m per event) is compensated by the shorter recurrence interval in that period (1500 yr), as compared to the earlier period of 45–16 k.y. (8 events, average slip of 1.4 m, and a recurrence interval of 3000 yr). The difference in slip per event between the two periods is statistically significant ($p < 0.002$ in the Mann–Whitney test, where p is the probability that the two samples are drawn from the same population).

Assuming an average slip rate of 5 mm/yr for the left-lateral motion along the DSF, the average cumulative normal slip rate in the southern Arava Valley of 0.5 mm/yr suggests that normal faulting is only $\sim 10\%$ of the total strike-slip motion in the past 45 k.y. This is supported by the calculated rake for small and large earthquakes along the DSF in modern times (Hofstetter *et al.*, 2003; Salamon *et al.*, 2003) and by the amount of transverse extension along the fault (e.g., Joffe and Garfunkel, 1987). A similar dip-slip to strike-slip ratio was observed in the northeastern Sea of Galilee basin (Marco *et al.*, 2005) and was estimated for the Dead

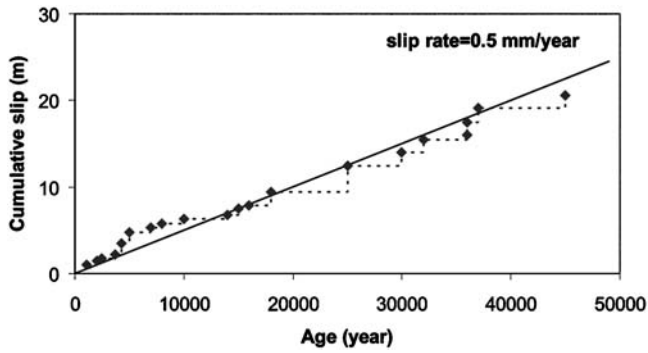


Figure 2. Cumulative normal slip versus time from the southern Arava Valley paleoseismic data (diamonds). The black line illustrates a slip rate of 0.5 mm/yr.

Sea basin using seismic refraction data (Ginzburg and Ben-Avraham, 1997).

The transformation of displacement detected in trenches across faults to earthquake magnitude was calculated using the regressions presented by Wells and Coppersmith (1994). The calculated magnitudes for all paleoearthquakes in the Arava Valley segment are in the range of $5.9 < M_w < 7.1$, with an average magnitude of M_w 6.5 for 16–1 k.y., and 6.8 for 45–16 k.y B.P. Because of the nature and inaccuracy

of the displacement-magnitude relation (Wells and Coppersmith, 1994), we assume an error in magnitude of ± 0.6 ($\sim 10\%$) for all paleoevents. The earthquake catalogs that are based on historical records report a single large earthquake ($M > 6$) that occurred in the year of 1068 A.D. in the southern Arava Valley (e.g., Guidoboni and Comastri, 2005; Zilberman *et al.*, 2005), which is included in the aforementioned record. Because of the remoteness of this desert area in ancient times, it is hard to find reliable historic evidence for earlier events. The instrumental data used in this study were taken from the Geophysical Institute of Israel earthquake catalog (see the Data and Resources section). As the catalog is complete for earthquakes with $M_L \geq 2$ only since 1983, we used instrumental data that were recorded between the years of 1983 and 2007. Figure 3a shows the calculated frequency–magnitude relation for the southern Arava Valley segment using the instrumental and paleoseismic records. The instrumental record includes 123 events and was divided into magnitudes between 2 and 2.9, 3 and 3.9, and 4 and 4.9. We found that the data points as retrieved from paleoseismic record for the southern Arava Valley segment lie on the linear extrapolation of the frequency–magnitude relation of the instrumental record, with a calculated b-value (the slope of the frequency–magnitude relations) of 1. This value is in agreement with $b = 0.96$ that was

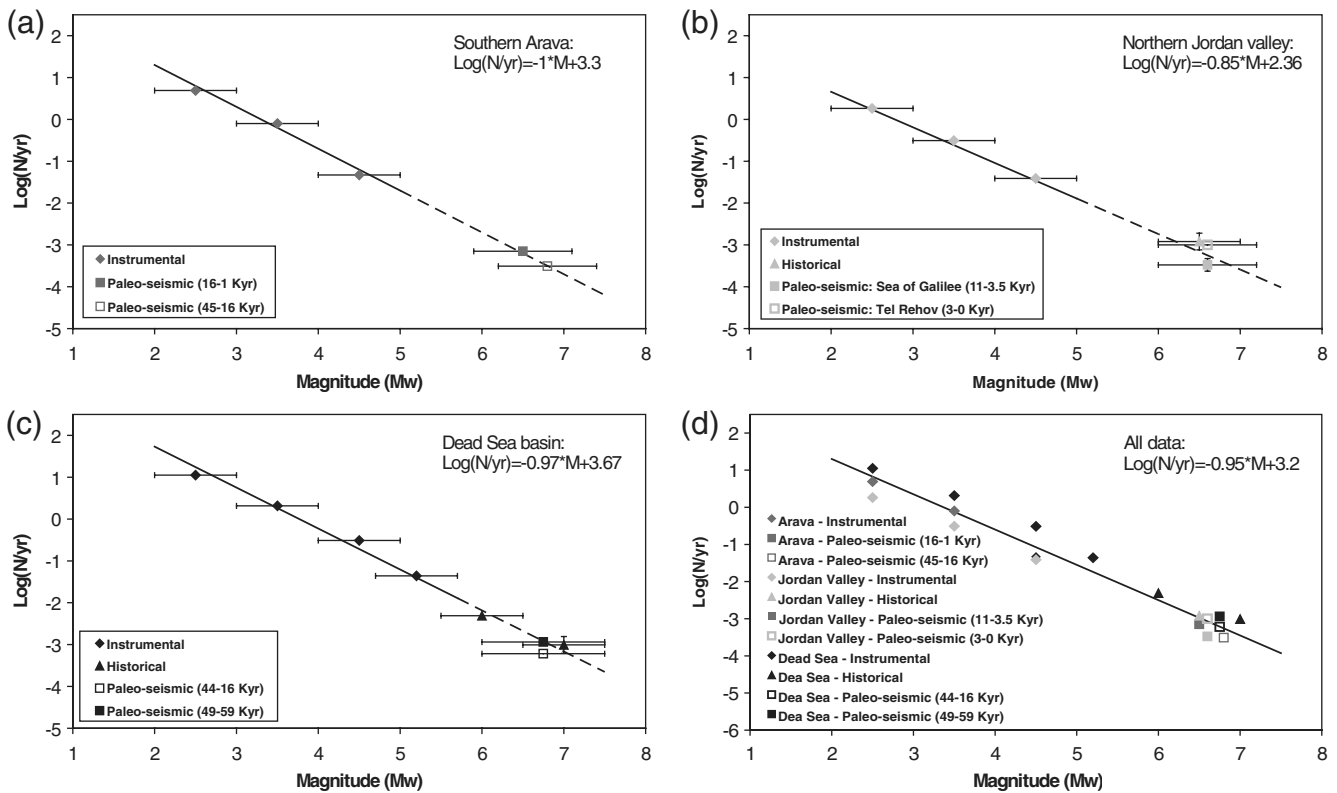


Figure 3. Frequency–magnitude relations for (a) the southern Arava Valley segment, (b) the northern Jordan Valley segment, (c) the Dead Sea basin, and (d) all three segments together using instrumental (diamonds), historical (triangles), and paleoseismic (squares) records. Black lines denote the regression curves for the instrumental record only (in [a]–[c]), and dashed lines denote its extrapolation. The black line in (d) denotes the best-fitting model for all data. Note that a b-value (the slope of the curve) of 0.95 can explain the whole data range for all three segments.

found for the DSF in Israel using instrumental data only (Shapira and Hofstetter, 2002).

Northern Jordan Valley

In the northern Jordan Valley, Late Quaternary paleoseismicity was deduced from normal offsets on faults detected in trenches in the same manner as in the southern Arava Valley segment. The paleoseismic data in this segment come from two different sites: one is east to the Sea of Galilee and the other is near the archeological site of Tel Rehov (Fig. 1). In the site east to the Sea of Galilee, three trenches were opened crossing three of the mapped north–south oriented faults between the western slopes of the Golan Heights and the eastern coast of the Sea of Galilee (Katz *et al.*, 2008). The data in this site include 2–4 different events between 11 and 3.5 k.y. B.P. In the Tel Rehov site, trenches were opened on a marginal mapped fault of the DSF, north to the archaeological site (Zilberman *et al.*, 2004). The data in this site include three different events in the past 3000 yr. Because of the small number of paleoevents, we did not estimate the slip rate for this segment. Using the regression presented by Wells and Coppersmith (1994), the calculated average magnitude for the paleoearthquakes in the northern Jordan Valley segment is M_w 6.6. Studies of macroseismic damage from historic events and archaeological evidence conclude that 1–3 large earthquake ($M_S > 6$) occurred in the northern Jordan Valley segment during the past 2000 yr (e.g., Ambraseys *et al.*, 1994; Guidoboni *et al.*, 1994; Marco *et al.*, 2003). According to these studies the earthquake of 749 (or 746) A.D. occurred along the Jordan Valley segment. However, it is not clear if the earthquakes of 363 and 1033 A.D. occurred along the Jordan Valley or the Dead Sea basin segments. The instrumental record for the northern Jordan Valley, which includes 59 events, was treated in a similar way as that of the Arava Valley segment. Figure 3b shows the calculated frequency–magnitude relation for the northern Jordan Valley segment using all data. Here also, the paleoseismic record lies on the linear extrapolation of the frequency–magnitude relation of the instrumental record, with a slightly lower b-value, namely 0.85. Figure 3b shows that the average recurrence interval for a large earthquake ($M \geq 6.5$) in this segment is ~ 1500 yr.

Dead Sea Basin

Late Pleistocene seismicity in the Dead Sea basin was deduced from the occurrence of 30 breccia beds (59,000–16,000 yr B.P.) within the lacustrine sediments of the Lisan Formation at the PZ1 section in Nahal Perazim (Fig. 1). These beds are considered to be seismites, having been induced by $M > 6$ earthquakes (Marco and Agnon, 1995; Marco *et al.*, 1996; Begin *et al.*, 2005). Based on these studies and assuming a maximum magnitude of 7.6 (see the Discussion section), all paleoseismic large events in the Dead Sea basin have magnitudes between 6 and 7.6.

Thus, we estimate an average magnitude for all these large earthquakes to be M 6.8 ± 0.8 . Two important differences between the record of this segment and that of the two former ones stem from the difference in the method of deduction of seismic activity. First, while in the Arava Valley and Jordan Valley segments the slip on faults records only earthquakes that actually took place on these faults, the Dead Sea seismites may record strong earthquakes that occurred at some distance north and south of the Dead Sea area. Second, while in the Arava Valley and Jordan Valley segments only the dip-slip component is recorded, the Dead Sea basin seismites recorded both dip- and strike-slip events.

Because of a hiatus in the Lisan Formation between 49 and 44 k.y. B.P. (Machlus *et al.*, 2000), which was not recognized by Marco *et al.* (1996), the paleoseismic data were divided into two periods: 59–49 and 44–16 k.y. B.P. The calculated recurrence interval for strong earthquakes (M 6.8 ± 0.8) in the period of 59–49 k.y. was found to be ~ 900 yr, while for 44–16 k.y. it was found to be ~ 1700 yr. The catalogs of historic earthquakes in the Dead Sea basin (e.g., Ambraseys *et al.*, 1994; Guidoboni *et al.*, 1994; Guidoboni and Comastri, 2005) are more complete than for the other segments; they include not only 1–3 large events ($6.5 < M_S < 7.5$), but also 9–10 medium events ($5.5 < M_S < 6.5$) that occurred since 31 B.C. (Table 1). Note, that we include the 1927 M_L 6.2 earthquake (Shapira *et al.*, 1993) in our historical record. The instrumental record for the Dead Sea basin includes 310 events of $2 \leq M_L \leq 5.2$. Figure 3c shows the calculated frequency–magnitude relation for the Dead Sea basin using the instrumental, historical, and paleoseismic data. As shown in Figure 3c the Dead Sea basin paleoseismic record also lies on the linear extrapolation of the frequency–magnitude relation of the instrumental record, with a calculated b-value of 0.97, which is close to the values of 1 and 0.85 that were found for the Arava Valley and the northern Jordan Valley segments, respectively. The Gutenberg–Richter (GR) relation for the combined record of Dead Sea basin shows that the higher seismic activity between 59 and 49 k.y. compared to the activity between 44 and 16 k.y. B.P., is an expected result from the a- and b-values of that relation. It appears from the combined record (Fig. 3c) that the calculated average recurrence interval for strong earthquakes ($M_w \geq 6.5$) in the Dead Sea basin is ~ 500 yr.

Discussion

We integrated paleoseismic, historical, and instrumental records of earthquakes in three different segments, 100 km apart, in order to detect the seismic activity of the DSF in the past 60,000 yr. Despite the limitations on the transformation of the paleoseismic and historic evidence to reliable estimates of earthquake magnitude, we adopt the assumption that the long-term characteristics of these records actually represent the trends of seismic behavior in the three segments. We further assume that the major seismic moment release is associated with the sinistral component of faulting

Table 1
Historic Earthquakes Used in This Study

Date	Main Source of Information	Estimated Magnitude [*]	Ruptured Segments [†]
31 B.C.	Guidoboni <i>et al.</i> (1994), Karcz (2004)	M	DS
363	Guidoboni <i>et al.</i> (1994)	L–	JV, DS
634	Guidoboni <i>et al.</i> (1994)	M	DS
659/660	Guidoboni <i>et al.</i> (1994)	M	DS
746 (or 749)	Guidoboni <i>et al.</i> (1994), Marco <i>et al.</i> (2003), Karcz (2004)	L–	JV
757 (or 749, or 750)	Guidoboni <i>et al.</i> (1994)	M	DS
1033	Ambraseys <i>et al.</i> (1994), Guidoboni and Comastri (2005)	L	JV, DS
1068	Ambraseys <i>et al.</i> (1994), Zilberman <i>et al.</i> (2005), Guidoboni and Comastri (2005)	L	AR
1105	Guidoboni and Comastri, 2005.	M	DS
c. 1150	Guidoboni and Comastri (2005)	M	DS
1293	Guidoboni and Comastri (2005).	L	DS
1458	Ambraseys <i>et al.</i> (1994), Klinger <i>et al.</i> (2000), Guidoboni and Comastri (2005)	M	DS
1557	Ambraseys and Karcz (1992)	M	DS
1927	Shapira <i>et al.</i> (1993)	M_L 6.2	DS

^{*}Estimated magnitude: M, moderate ($5.5 < M_S < 6.5$); L, large ($6.5 < M_S < 7.5$).

[†]Ruptured segment: AR, southern Arava Valley; DS, Dead Sea basin; JV, Jordan Valley.

along the DSF. We found that the GR relation explains the observed data rather well, with calculated b -values between 0.85 and 1 for the three segments (Fig. 3a–c) and with $b = 0.95$ for all data (Fig. 3d). These values are in agreement with frequency–magnitude relations observed in other major strike-slip faults in the world (e.g., Evernden, 1970; Shi and Bolt, 1982; Bakun, 1999). Note that for small magnitude earthquakes (instrumental record) the seismic activity in the Dead Sea basin is higher than in the other segments (Fig. 3d). For large magnitude earthquakes, however, our historical and paleoseismic records suggest that the seismic activity in all segments may be similar. It should also be noted that an extrapolation of the GR relation beyond the data limits would not be justified because not a single estimation has been suggested of an earthquake stronger than $M > 7.6$ along the DSF in Israel in the past 60,000 yr. This observation is compatible with the relatively short segments that characterize the DSF in Israel (~60 km long; ten Brink *et al.*, 1999). Stronger earthquakes may possibly occur on the Yammuneh restraining bend in Lebanon.

Both the southern Arava Valley and Dead Sea basin paleoseismic data show some temporal variations in seismic activity, the origins of which are not clear. For the southern Arava Valley segment, the average recurrence interval and magnitude between 45 and 16 k.y. B.P. are ~3000 yr and 6.8, while between 16 and 1 k.y. B.P. they are ~1500 yr and 6.5, respectively. For the Dead Sea basin, the average recurrence interval for $M > 6.8 \pm 0.8$ earthquakes between 59 and 49 k.y. B.P. is ~900 yr, while between 44 and 16 k.y. B.P. it is ~1700 yr. We suggest that these variations do not result from changes in slip rate along the DSF, as can be deduced from the fact that the average slip rate of 5 mm/yr along the DSF as calculated for a time window of 20 m.y. is the same as the current slip rate as detected by GPS measurements during several years. This conclusion is also supported by the observation that a constant slip rate

of 0.5 mm/yr can explain all normal faulting during the past 45,000 yr in the southern Arava Valley (Fig. 2). At any rate, the temporal variation in seismic activity, compared to the accuracy of the data, is small, and the whole data set is still well represented by a GR relation (Fig. 3d).

The GR relation, with power-law distribution of earthquake statistics, is an end-member mode that was proposed to explain earthquake distribution. The other end member is the characteristic earthquake mode, with more earthquakes closer to the maximum magnitude than expected by GR relations (Schwartz and Coppersmith, 1984). As shown by Lyakhovskiy *et al.* (2001), the ratio between the timescale of fault healing and loading provides a guideline for understanding different fault evolution patterns and earthquake statistics. Fault systems with a long memory (high loading rate) tend to produce high localization and frequency–magnitude relations that are typical of characteristic earthquake statistics. Conversely, fault systems with a short memory (low loading rate) tend to produce a disordered and diffuse fault system with GR distributions of earthquakes. This correlation between fault geometry and earthquake statistics is in agreement with the seismological and field observations (e.g., Wesnousky, 1994; Stirling *et al.*, 1996). Different segments of the San Andreas fault show the two modes. The frequency–magnitude relation in southern California is in accord with the characteristic earthquake mode (Wesnousky, 1994), while the observed seismic data for northern and central California can be explained through the GR relation (Shi and Bolt, 1982; Bakun, 1999). We suggest that because the loading rate in the DSF is an order of magnitude lower than that of the San Andreas fault and because at least part of the San Andreas fault operates according to the GR relation, the latter is more compatible with the tectonic setting of the DSF. The fact that the GR relation can explain the seismic behavior of the DSF during the past 60,000 yr suggests that this is a stable mode in the seismicity of the DSF.

Data and Resources

Paleoseismic and historical data sets used in this article came from published sources listed in the references. The modern (instrumental) seismic data can be obtained from the Geophysical Institute of Israel earthquake catalog (www.gii.gov.il, last accessed September 2007).

Acknowledgments

We thank V. Lyakhovsky, Y. Ben-Zion, and G. Shamir for useful discussions. We also would like to thank the Editor, Diane I. Doser, and one anonymous reviewer for their constructive reviews.

References

- Ambraseys, N. N., and I. Karcz (1992). The earthquake of 1546 in the Holy Land, *Terra Nova* **4**, 253–262.
- Ambraseys, N. N., C. P. Melville, and R. D. Adams (1994). *The Seismicity of Egypt, Arabia and the Red Sea: A Historical Review*, Cambridge University Press, Cambridge.
- Amit, R., J. B. J. Harrison, and Y. Enzel (1995). Use of soils and colluvial deposits in analyzing tectonic events—the southern Arava rift, Israel, *Geomorphology* **12**, 91–107.
- Amit, R., E. Zilberman, Y. Enzel, and N. Porat (2002). Paleoseismic evidence for time dependency of seismic response on a fault system in the southern Arava Valley, Dead Sea rift, Israel, *Geol. Soc. Am. Bull.* **114**, 192–206.
- Bakun, W. H. (1999). Seismic activity of the San Francisco Bay region, *Bull. Seismol. Soc. Am.* **89**, 764–784.
- Bartov, Y., and A. Sagy (2004). Late Pleistocene extension and strike-slip in the Dead Sea basin, *Geol. Mag.* **141**, 565–572.
- Begin, Z. B., and G. Steinitz (2005). Temporal and spatial variations of microearthquake activity along the Dead Sea fault, 1984–2004, *Israel J. Earth Sci.* **54**, 1–14.
- Begin, Z. B., D. M. Steinberg, G. A. Ichinose, and S. Marco (2005). A 40,000 years unchanging the seismic regime in the Dead Sea rift, *Geology* **33**, 257–260.
- Daëron, M., L. Benedetti, P. Tapponnier, A. Sursock, and R. C. Finkel (2004). Constraints on the post 25-ka slip rate of the Yammouneh fault (Lebanon) using *in situ* cosmogenic ³⁶Cl dating of offset limestone-clast fans, *Earth Planet. Sci. Lett.* **227**, 105–119.
- El-Isa, Z. H., and H. Mustafa (1986). Earthquake deformations in the Lisan deposits and seismotectonic implications, *Geophys. J. R. Astron. Soc.* **86**, 413–424.
- Evernden, J. F. (1970). Study of regional seismicity and associated problems, *Bull. Seismol. Soc. Am.* **60**, 393–446.
- Ferry, M., M. Meghraoui, N. A. Karaki, M. Al-Taj, H. Amoush, S. Al-Dhaisat, and M. Barjous (2007). A 48-kyr-long slip rate history for the Jordan Valley segment of the Dead Sea fault, *Earth Planet. Sci. Lett.* **260**, 394–406.
- Garfunkel, Z., I. Zak, and R. Freund (1981). Active faulting in the Dead Sea rift, *Tectonophysics* **80**, 1–26.
- Ginat, H., Y. Enzel, and Y. Avni (1998). Translocation of Plio-Pleistocene drainage system along the Dead Sea Transform, south Israel, *Tectonophysics* **284**, 151–160.
- Ginzburg, A., and Z. Ben-Avraham (1997). A seismic reflection study of the north basin of the Dead Sea, Israel, *Geophys. Res. Lett.* **24**, 2063–2066.
- Gomez, F., G. Karam, M. Khawlie, S. McClusky, P. Vernant, R. Reilinger, R. Jaafar, C. Tabet, K. Khair, and M. Barazangi (2007). Global Positioning System measurements of strain accumulation and slip transfer through the restraining bend along the Dead Sea fault system in Lebanon, *Geophys. J. Int.* **168**, 1021–1028.
- Guidoboni, E., and A. Comastri (2005). *Catalogue of Earthquakes and Tsunamis in the Mediterranean Area from the 11th to the 15th Century*, Istituto Nazionale di Geofisica e Vulcanologia–Storia Geofisica Ambiente (INGV-SGA), Italy.
- Guidoboni, E., A. Comastri, and G. Traina (1994). *Catalogue of Ancient Earthquakes in the Mediterranean Area up to the 10th Century* INGV-SGA, Italy.
- Hofstetter, A., H. K. Thio, and G. Shamir (2003). Source mechanisms of the 22/11/1995 Gulf of Aqaba earthquake and its aftershock sequence, *J. Seism.* **7**, 99–114.
- Joffe, S., and Z. Garfunkel (1987). Plate kinematics of the circum Red Sea—A re-evaluation, *Tectonophysics* **141**, 5–22.
- Karcz, I. (2004). Implications of some early Jewish sources for estimates of earthquake hazard in the Holy Land, *Ann. Geophys.* **47**, 759–792.
- Katz, O., R. Amit, G. Yagoda, Y. H. Hatzor, N. Porat, and H. Hecht (2008). Seismic history of the southeastern Sea of Galilee margins, Dead Sea rift, Israel, *Geophys. Res. Abstr.* **10**, EGU2008-A-11834.
- Klinger, Y., J. P. Avouac, N. Abou-Karaki, L. Dorbath, D. Bourles, and J. L. Reyss (2000). Slip rate on the Dead Sea transform fault in northern Arava Valley (Jordan), *Geophys. J. Int.* **142**, 755–768.
- Le Beon, M., Y. Klinger, A. Q. Amrat, A. Agnon, L. Dorbath, G. Baer, J.-C. Ruegg, O. Charade, and O. Mayyas (2008). Slip rate and locking-depth from GPS profiles across the southern Dead Sea Transform, *J. Geophys. Res.* **113**, B11403, doi 10.1029/2007JB005280.
- Leonard, G., D. M. Steinberg, and N. Rabinowitz (1998). An indication of time-dependent seismic behaviour—An assessment of paleoseismic evidence from the Arava fault, Israel, *Bull. Seismol. Soc. Am.* **88**, 767–776.
- Lyakhovsky, V., Y. Ben-Zion, and A. Agnon (2001). Fault evolution and seismicity patterns in a rheologically layered half-space, *J. Geophys. Res.* **106**, 4103–4120.
- Machlus, M., Y. Enzel, S. L. Goldstein, S. Marco, and M. Stein (2000). Reconstructing low levels of Lake Lisan by correlating fan-delta and lacustrine deposits, *Quat. Inter.* **73/74**, 137–144.
- Mahmoud, S., R. Reilinger, S. McClusky, P. Vernant, and A. Tealeb (2005). GPS evidence for northward motion of the Sinai Block: Implications for East Mediterranean tectonics, *Earth Planet. Sci. Lett.* **238**, 217–224.
- Marco, S., and A. Agnon (1995). Prehistoric earthquake deformations near Masada, Dead Sea graben, *Geology* **23**, 695–698.
- Marco, S., M. Hartal, N. Hazan, L. Lev, and M. Stein (2003). Archaeology, history, and geology of the 749 AD earthquake, Dead Sea Transform, *Geology* **31**, 665–668.
- Marco, S., T. K. Rockwell, A. Heimann, U. Frieslander, and A. Agnon (2005). Late Holocene slip of the Dead Sea Transform revealed in 3D palaeoseismic trenches on the Jordan Gorge segment, *Earth Planet. Sci. Lett.* **234**, 189–205.
- Marco, S., M. Stein, A. Agnon, and H. Ron (1996). Long term earthquake clustering: A 50,000 year paleoseismic record in the Dead Sea graben, *J. Geophys. Res.* **101**, 6179–6192.
- McClusky, S., R. Reilinger, S. Mahmoud, D. B. Sari, and A. Tealeb (2003). GPS constraints on Africa (Nubia) and Arabia plate motions, *Geophys. J. Int.* **155**, 126–138.
- Meghraoui, M., F. Gomez, R. Sbeinati, J. V. der Woerd, M. Mouty, A. N. Darkal, Y. Radwan, I. Layyous, H. A. Najjar, R. Darawchah, F. Hijazi, R. Al-Ghazzi, and M. Barazangi (2003). Evidence for 830 years of seismic quiescence from palaeoseismology, archaeoseismology, and historical seismicity along the Dead Sea fault in Syria, *Earth Planet. Sci. Lett.* **210**, 35–52.
- Migowski, C., A. Agnon, R. Bookman, J. F. W. Negendank, and M. Stein (2004). Recurrence pattern of Holocene earthquakes along the Dead Sea transform revealed by varve-counting and radiocarbon dating of lacustrine sediments, *Earth Planet. Sci. Lett.* **222**, 301–314.
- Niemi, T. M., H. Zhang, M. Atallah, and B. J. Harrison (2001). Late Pleistocene and Holocene slip rate of the northern Wadi Arava fault, Dead Sea Transform, Jordan, *J. Seism.* **5**, 449–474.
- Ostrovsky, E. (2001). The G1 GPS geodetic-geodynamic reference network: Final processing results, *Isr. J. Earth Sci.* **50**, 29–37.

- Ostrovsky, E. (2005). The G1 GPS geodetic-geodynamic reference network: Results of the G1 GPS surveying campaigns in 1996/1997 and 2001/2002, Technical Project Report, Survey of Israel, 52 pp.
- Salamon, A., A. Hofstetter, Z. Garfunkel, and H. Ron (2003). Seismotectonics of the Sinai subplate—The eastern Mediterranean region, *Geophys. J. Int.* **155**, 149–173.
- Schwartz, D. P., and K. J. Coppersmith (1984). Fault behavior and characteristic earthquakes: Examples from the Wasatch and San Andreas fault zones, *J. Geophys. Res.* **89**, 5681–5698.
- Shapira, A., and A. Hofstetter (2002). Seismicity parameters of seismogenic zones, *Geophys. Inst. Isr. Rept.*, 592/230/02.
- Shapira, A., R. Avni, and A. Nur (1993). Note: A new estimate for the epicenter of the Jericho earthquake of 11 July 1927, *Isr. J. Earth Sci.* **42**, 93–96.
- Shi, Y., and B. A. Bolt (1982). The standard error of the magnitude–frequency b-value, *Bull. Seismol. Soc. Am.* **72**, 1677–1687.
- Steady, S., J. Gomberg, and M. Cocco (2005). Introduction to special section: Stress transfer, earthquake triggering, and time-dependent seismic hazard, *J. Geophys. Res.* **110**, 1–12.
- Stirling, M. W., S. W. Wesnousky, and K. Shimazaki (1996). Fault trace complexity, cumulative slip, and the shape of the magnitude–frequency distribution for strike-slip faults: A global survey, *Geophys. J. Int.* **124**, 833–868.
- ten Brink, U., M. Rybakov, A. Al-Zoubi, M. Hassouneh, A. Batayneh, U. Frieslander, V. Goldschmidt, M. Daoud, Y. Rotstein, and J. K. Hall (1999). The anatomy of the Dead Sea plate boundary: Does it reflect continuous changes in plate motion?, *Geology* **27**, 887–980.
- Wdowinski, S., Y. Bock, G. Baer, L. Prawirodirdjo, N. Bechor, S. Naaman, R. Knafo, Y. Forrai, and Y. Melzer (2004). GPS measurements of current crustal movements along the Dead Sea fault, *J. Geophys. Res.* **109**, 1–16.
- Wells, D. L., and K. J. Coppersmith (1994). New empirical relationships among magnitudes, rupture length, rupture width, rupture area, and surface displacement, *Bull. Seismol. Soc. Am.* **84**, 974–1002.
- Wesnousky, S. G. (1994). The Gutenberg–Richter or characteristic earthquake distribution, which is it?, *Bull. Seismol. Soc. Am.* **84**, 1940–1959.
- Zilberman, E., R. Amit, I. Bruner, and Y. Nahmias (2004). Neotectonic and paleoseismic study—Bet Shean Valley, *Geol. Survey Isr. Rept.*, GSI/15/04.
- Zilberman, E., R. Amit, A. Heimann, and N. Porat (2000). Changes in Holocene paleoseismic activity in the Hula pull-apart basin, Dead Sea rift, northern Israel, *Tectonophysics* **321**, 237–252.
- Zilberman, E., R. Amit, N. Porat, Y. Enzel, and U. Avner (2005). Surface ruptures induced by the devastating 1068 AD earthquake in the southern Arava Valley, Dead Sea rift, Israel, *Tectonophysics* **408**, 79–99.

The Geological Survey of Israel
 30 Malkhe Israel Street
 Jerusalem 95501, Israel
 yariv@gsi.gov.il
 (Y.H., R.A., Z.B.B., O.K., A.S., E.Z., N.P.)

Department of Geophysics and Planetary Physics
 Tel Aviv University
 Tel Aviv 69978, Israel
 (S.M.)

Manuscript received 31 July 2008